

LATERAL-DIRECTIONAL HANDLING AND FLYING QUALITIES ASSESSMENT OF A BLENDED WING BODY (BWB) ACFA 2020 CONFIGURATION

Mushfiqul Alam[1], Julien Renault[1], Martin Hromcik[2], & Tomas Hanis[2]
[1] Centre for Aeronautics Power and Propulsion, Faculty of Engineering and Applied Science (FEAS), Cranfield University, United Kingdom
mushfiqul.alam@cranfield.ac.uk
[2] Department of Control Engineering, Faculty of Electrical Engineering, Czech Technical University in Prague, Czech Republic
xhromcik@fel.cvut.cz, tomas.hanis@fel.cvut.cz

Abstract

The blended wing body (BWB) configuration offers significant potential for future transport aircraft through improved aerodynamic efficiency, reduced fuel burn, and opportunities for lower external noise. However, its tailless architecture and large flexible lifting surface introduce important challenges in lateral–directional flying qualities, gust response, aeroelastic coupling, and passenger ride comfort. This paper investigates the ACFA 2020 flexible BWB configuration using a previously developed lateral–directional active control framework based on robust H_∞ feedback control combined with feedforward load alleviation. The study evaluates the aircraft response under representative manoeuvre and disturbance conditions, with particular focus on a 60° bank-angle manoeuvre and a severe lateral gust. The antisymmetric wing acceleration parameter $N_{z_{lat.law}}$ is used to assess gust-induced flexible structural excitation, while passenger comfort is evaluated at multiple cabin locations using the BS 6841 standard. Both low-frequency motion sickness sensitivity and higher-frequency whole-body vibration exposure are considered using frequency-weighted RMS acceleration metrics. The results show that lateral gust disturbances significantly amplify the antisymmetric bending response of the flexible BWB aircraft, particularly under combined manoeuvre-and-gust conditions. Passenger comfort levels vary strongly across the distributed cabin, with outboard and aft locations exhibiting the highest sensitivity to motion sickness and whole-body vibration. The findings highlight the importance of considering passenger ride comfort as an integrated design driver for future flexible BWB aircraft, alongside flying qualities, active control design, and structural load alleviation.

Keywords: blended wing body aircraft, flexible aircraft, flying quality, passenger comfort, lateral–directional flight control

1. Introduction

1.1 Sustainable Aviation and Blended Wing Body Configurations

The aviation sector faces increasing pressure to reduce environmental impact while maintaining performance and long-range transport capability. Alongside developments in sustainable aviation fuels, hybrid-electric propulsion and hydrogen-based concepts, unconventional aircraft configurations are being explored to deliver step-change improvements in aerodynamic efficiency [1,2].

The Blended Wing Body (BWB) is one of the most promising configurations, as its integrated wing–fuselage layout reduces wetted area and form drag while improving lift-to-drag ratio [3]. It also offers potential noise benefits through engine shielding and optimized high-lift device integration [4]. However, its large span, structural flexibility and tailless architecture introduce significant stability, control and aeroelastic challenges.

For BWB aircraft, passenger comfort is also a critical design consideration, as occupants are distributed across a wide flexible lifting surface and may be more directly exposed to manoeuvre- and gust-induced vibrations. This motivates the use of active flight control systems capable of simultaneously addressing flying qualities, load alleviation and ride comfort.

https://doi.org/10.71945/icas2026_0630

1.2 Stability and Control Challenges of Flexible BWB Aircraft

Despite their aerodynamic and environmental advantages, BWB aircraft present significant stability and control challenges due to their tailless architecture and large flexible lifting surface. In comparison with conventional tube-and-wing aircraft, BWB configurations typically exhibit reduced directional stability and yaw damping, leading to poor Dutch roll characteristics and strong lateral–directional coupling [3,5]. Previous studies have shown that reduced values of the directional stability derivative, C_{n_β}, the yaw damping derivative, C_{n_r}, and the roll damping derivative, C_{l_p}, can degrade lateral–directional handling qualities, particularly at low-speed flight conditions [6,7].

In addition to rigid-body stability deficiencies, the large span and reduced structural stiffness of BWB aircraft introduce significant aeroelastic effects. Manoeuvres and atmospheric disturbances can strongly excite flexible structural modes, leading to coupling between rigid-body motion and structural dynamics [4,8]. Such interactions can amplify passenger accelerations and structural loads, particularly in outboard cabin regions located far from the aircraft centreline.

To address these challenges, the Active Control for Flexible Aircraft (ACFA 2020) programme investigated advanced active control concepts combining stability augmentation, load alleviation, and vibration suppression [8]. Modern control approaches including robust H_∞ control, LPV methods, and feedforward disturbance rejection strategies were explored to improve flying qualities while mitigating gust-induced structural excitation.

1.3 ACFA 2020 Programme and Active Control Concept

The Active Control for Flexible Aircraft (ACFA 2020) project was a European research programme aimed at developing advanced active control technologies for future flexible transport aircraft [8]. The project focused on two unconventional aircraft configurations, including a blended wing body (BWB) transport aircraft designed for approximately 450 passengers. A major objective of the programme was to investigate how modern flight control techniques could simultaneously improve flying qualities, structural load alleviation, and passenger ride comfort.

The ACFA 2020 BWB configuration features a highly blended lifting surface with distributed control effectors, including elevons, split ailerons, winglet-mounted rudders, and crocodile flaps used for yaw stabilization and control allocation [4]. Due to the reduced directional stability associated with tailless configurations, active flight control systems play a critical role in ensuring acceptable lateral–directional handling qualities throughout the flight envelope. The ACFA 2020 BWB configuration and control surface allocation are shown in Figure 1.

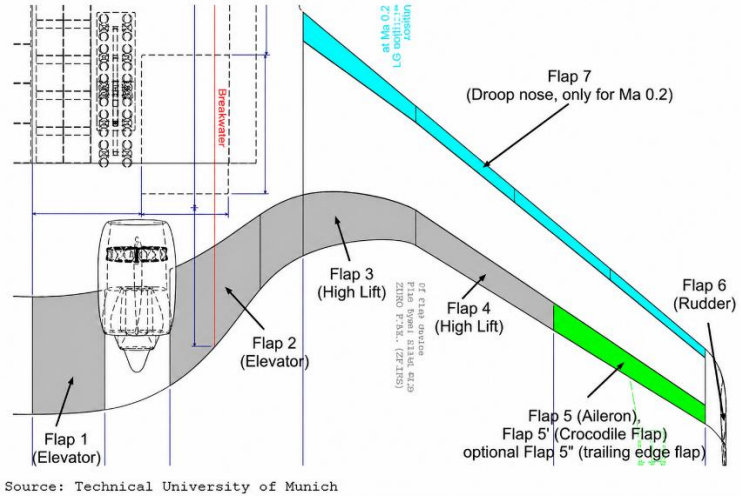


Figure 1. The ACFA 2020 BWB aircraft configuration and control surface allocation, adapted from [4].

To support controller development, high-fidelity aeroelastic models of the aircraft were generated and subsequently reduced into lower-order representations suitable for control synthesis and robustness analysis [8]. The models included flexible structural dynamics, actuator and sensor dynamics, atmospheric disturbances, and uncertainty representations. In total, multiple flexible modes were retained to capture the interaction between rigid-body motion and structural response.

The ACFA control architecture combined feedback stabilization with feedforward load alleviation strategies. Several modern control approaches were investigated within the programme, including robust H_∞control, LPV control, and adaptive control methods [8]. The overall objective was not only to

https://doi.org/10.71945/icas2026_0630

satisfy flying qualities requirements, but also to mitigate gust-induced structural excitation and improve passenger comfort through active vibration suppression.

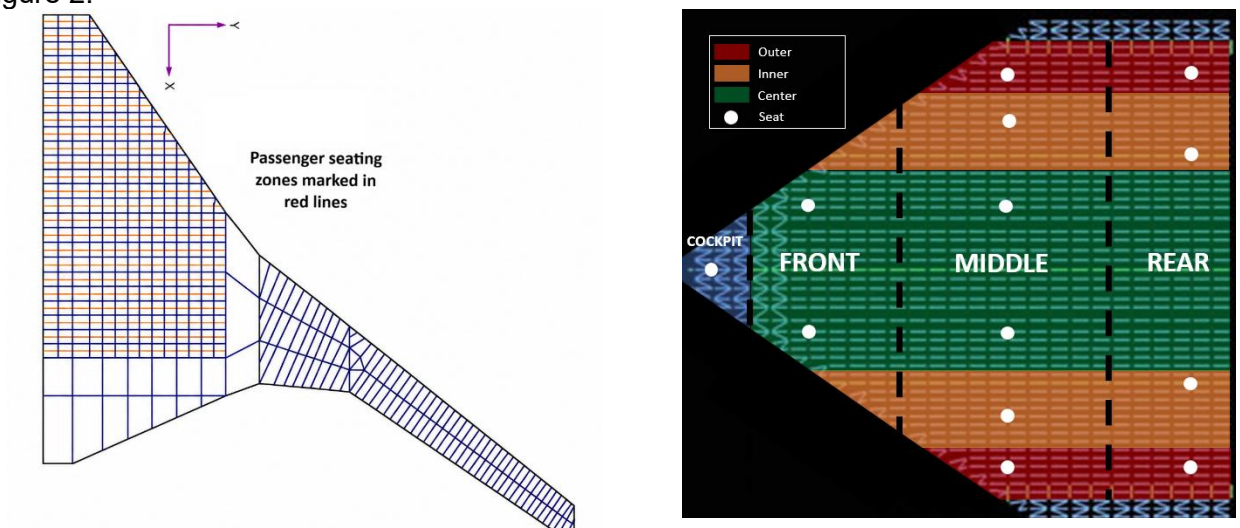
1.4 Ride Comfort in Flexible BWB Aircraft

Passenger ride comfort represents a significant challenge for future blended wing body aircraft due to the distributed cabin arrangement across a large flexible lifting surface. Unlike conventional tube-and-wing aircraft, where most passengers are located close to the fuselage centreline, BWB passengers may be positioned far from the aircraft roll axis and closer to structurally flexible wing regions. Consequently, atmospheric disturbances, manoeuvre-induced loads, and aeroelastic deformations can produce substantial spatial variations in vibration exposure throughout the cabin.

The combination of large structural flexibility and distributed passenger seating introduces strong coupling between rigid-body motion, flexible structural dynamics, and human vibration exposure. In particular, gust excitation may significantly amplify low-frequency structural modes, leading to increased passenger accelerations at outboard cabin locations. Such effects are especially important for lateral–directional manoeuvres, where rolling motion and asymmetric structural deformation may generate discomfort levels that differ considerably across the cabin.

Previous research on flexible BWB aircraft has primarily focused on flying qualities, stability augmentation, and structural load alleviation [3,4,8]. However, comparatively fewer studies have investigated the resulting passenger ride comfort characteristics under realistic manoeuvre and gust conditions. As a result, the interaction between active flight control systems, gust-induced aeroelastic response, and distributed cabin comfort remains insufficiently understood for large flexible transport aircraft.

Human sensitivity to vibration depends strongly on both frequency content and excitation direction [9,10]. Low-frequency vibrations are associated with motion sickness effects, while higher-frequency whole-body vibrations contribute to discomfort and fatigue. To evaluate these effects, standards such as ISO 2631 [11] and BS 6841 [12] are commonly employed. In the present study, the BS 6841 standard was selected due to its suitability for multi-axial vibration assessment in aerospace applications [13]. The passenger seating zones used for the ride comfort assessment are shown in Figure 2.



(a) Passengers seating distribution on the BWB aircraft [4].

(b) Position of evaluated passenger seats for comfort evaluation, adapted from [4].

Figure 2. Passenger seating zones and representative cabin locations used for ride comfort evaluation, adapted from [4]. Figures not to scale.

1.5 Scope and Contribution of the Present Work

This paper investigates the lateral–directional flying qualities and passenger ride comfort characteristics of the ACFA 2020 flexible blended wing body configuration under representative manoeuvre and gust disturbance conditions. Particular attention is given to the interaction between active flight control, aeroelastic response, and distributed cabin vibration exposure.

https://doi.org/10.71945/icas2026_0630

A robust H_∞-based feedback controller combined with a feedforward load alleviation strategy is evaluated for lateral–directional manoeuvres involving significant rolling motion and gust excitation. The study focuses on the resulting structural response and its influence on passenger comfort at multiple cabin locations distributed across the lifting surface.

Passenger ride comfort is assessed using the BS 6841 standard [12], considering both low-frequency motion sickness sensitivity and higher-frequency whole-body vibration exposure. The analysis highlights the spatial variability of ride quality throughout the cabin and identifies the passenger regions most sensitive to gust-induced structural excitation.

The rest of the paper is organized as follows. Section 2 introduces the ACFA 2020 BWB aircraft model, its flexible dynamic characteristics, and the lateral–directional active control framework used in this study. Section 3 describes the handling qualities and passenger ride comfort assessment methodology, including the BS 6841 comfort criteria, passenger-seat evaluation locations, and manoeuvre and gust definitions. Section 4 presents the simulation setup and results, including gust-induced flexible response, passenger comfort assessment, and the influence of centre-of-gravity position and fuel loading. Finally, Section 5 summarizes the main conclusions and discusses implications for future flexible BWB aircraft design.

2 Aircraft Model and Prior Active Control Framework

2.1 Aircraft Model Description

The aircraft considered in this study is the ACFA 2020 blended wing body transport configuration, originally developed within the European Active Control for Flexible Aircraft programme. The configuration represents a large passenger BWB aircraft, with approximately 450 passengers and two rear-mounted turbofan engines and has been used in previous studies on flexible aircraft modelling, control design and fuel-management optimisation [4,14].

The ACFA BWB exhibits the key dynamic characteristics associated with large flexible tailless aircraft: reduced static stability margins, limited control moment arms, strong lateral–directional coupling, and significant interaction between rigid-body and flexible structural modes. These features make the configuration particularly suitable for investigating active control concepts that address flying qualities, structural load alleviation and passenger comfort.

The present work builds on the lateral–directional active control framework previously developed within the ACFA programme. In that framework, robust feedback control and feedforward command shaping were used to improve aircraft response while reducing structural excitation. Rather than redesigning the aircraft model or controller, this paper uses the established ACFA BWB model and controller architecture as the basis for assessing gust-induced flexible response and passenger ride comfort across distributed cabin locations.

2.2 Lateral–Directional Active Control Framework

The flexible nature of the ACFA 2020 blended wing body aircraft introduces strong coupling between rigid-body motion and structural dynamics, making conventional lateral–directional flight control design particularly challenging. Initial investigations using classical rigid-body stability augmentation approaches showed that although rigid-body modes could be stabilized, flexible structural modes were easily excited, leading to degraded closed-loop behaviour and potential spillover effects.

In particular, the proximity between the flexible structural modes and the rigid-body lateral–directional dynamics complicates the application of conventional loop-by-loop control techniques. Furthermore, the aircraft exhibits strong coupling between roll and yaw motion, including adverse yaw behaviour associated with the lateral–directional aerodynamic derivatives and distributed control surface arrangement. The difference between the rigid and flexible roll-rate response is illustrated in Figure 3.

https://doi.org/10.71945/icas2026_0630

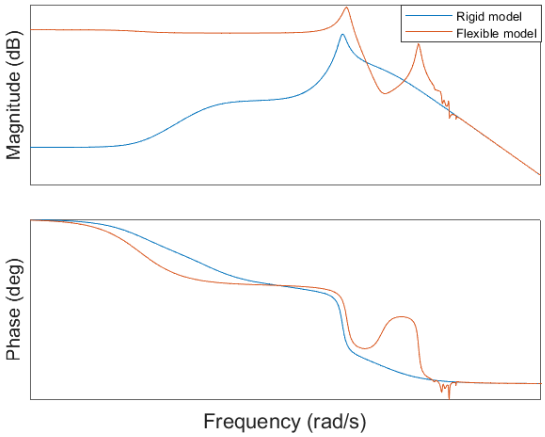


Figure 3. Bode plots of $p(s)/\delta_a(s)$, comparing the roll-rate-to-aileron transfer function of the rigid-body and flexible aircraft models. Axes removed for confidentiality.

Previous investigations performed within the ACFA 2020 programme therefore adopted advanced robust control approaches capable of simultaneously addressing flying qualities, structural load alleviation, and passenger comfort requirements [4,8]. The present work builds upon this previously developed active control framework for the assessment of gust-induced flexible response and passenger ride comfort.

2.2.1 *Lateral–Directional Control Objectives*

The lateral–directional control system was designed to satisfy robustness, tracking, disturbance rejection, and manoeuvre load alleviation requirements across multiple mass configurations. In addition to stabilizing the flexible aircraft dynamics, the controller was required to mitigate gust-induced structural excitation while maintaining acceptable roll and sideslip response characteristics.

Table 1. Lateral-directional design objectives.

General and tracking specifications	
Dutch Roll (DR) mode	$\zeta_{DR} > 0.7$, ω_{DR} unchanged
Decoupling	Generate inputs with high coupling to roll and sideslip angles and low cross-coupling.
Roll angle ϕ	DC gain similar for all mass cases, rise time to 90% in $t_{rise} < 7$ s, max. 5% overshoot.
Sideslip angle β	DC gain similar for all mass cases, $t_{rise} < 5$ s
Robustness	Stable controller, Robust Stability (RS) and Robust Performance (RP) for all mass cases.
Disturbance rejection specifications	
Lateral gust rejection	Minimize the influence of lateral gust on roll, sideslip, and lateral acceleration, while obeying the tracking specifications above. Moreover, the loads must not be increased.
Manoeuvre loads alleviation specifications	
Manoeuvre loads alleviation	Robustly minimize sizing *Fz*, *Mx*, and *My* (shear, bending and torsional) loads along the wing in 60° roll manoeuvres.

Unlike conventional transport aircraft, the roll response requirements were intentionally relaxed to reduce structural loading and improve passenger ride comfort. In particular, the target roll response was selected to achieve a bank-angle rise time below 7 seconds while limiting overshoot and minimizing excitation of the dominant flexible modes. Although this response does not satisfy the conventional MIL-F-8785C roll agility criterion, the reduced manoeuvre aggressiveness limits the vertical accelerations experienced throughout the cabin.

To capture asymmetric structural excitation during rolling manoeuvres and gust encounters, the ACFA framework introduced the antisymmetric wingtip acceleration parameter:

$$N_{z_{lat.law}} = N_{z,r.wingtip} - N_{z,l.wingtip} \tag{1}$$

where $N_{z_{r.wingtip}}$ and $N_{z_{l.wingtip}}$ represent the vertical accelerations at the right and left wingtips, respectively. This parameter provides a direct measure of antisymmetric bending activity within the

https://doi.org/10.71945/icas2026_0630

flexible airframe. The inner and middle ailerons (FL3 and FL4) were selected for lateral control implementation because their aerodynamic effectiveness remains consistent across the flight envelope, unlike the outer ailerons (FL5), which exhibit control reversal effects under certain conditions [4,15–17].

2.2.2 *Robust H_∞ Feedback and Feedforward Control Designs*

The lateral–directional flight control system used in this study consists of a robust multi-input multi-output (MIMO) feedback controller combined with a feedforward command-shaping controller. The feedback controller was synthesized using an H_∞ mixed-sensitivity framework in order to provide disturbance rejection, robustness to mass-case variations, and attenuation of flexible structural modes [4]. In particular, the controller was designed to reduce the response near the dominant antisymmetric bending frequencies, especially the first and second wing bending modes.

The robust feedback synthesis may be expressed in compact form as:

$$K(s) = \arg\min_{K} \| T_{zw}(s;K) \|_\infty \tag{2}$$

where $K(s)$ is the H_∞ feedback controller and $T_{zw}(s;K)$ is the closed-loop transfer function from exogenous inputs w to regulated outputs z. The output vector (z) contains the quantities to be controlled or minimized, including tracking errors, control effort, and structural-response-related outputs. Frequency weighting functions were used to shape the closed-loop response, particularly around the dominant flexible mode frequencies.

The measured feedback vector supplied to the H_∞ controller is:

$$y_m(s) = \begin{bmatrix} \beta(s) \\ \phi(s) \\ p(s) \\ r(s) \\ N_{z_{lat.law}}(s) \end{bmatrix} \tag{3}$$

where β is sideslip angle, $\phi$is bank angle, $p$is roll rate, r is yaw rate, and $N_{z_{lat.law}}$ is the antisymmetric wing acceleration signal.

In addition to the feedback controller, a feedforward controller was implemented to improve ride comfort and reduce structural loading during roll manoeuvres. The feedforward controller was synthesized using a convex optimization framework based on linear matrix inequalities (LMI), enabling time-domain and frequency-domain requirements to be incorporated directly into the design. These requirements include the 7 s bank-angle rise time, sideslip decoupling, overshoot limitations, and load-alleviation objectives.

The combined feedback–feedforward control law can be written as:

$$u(s) = K(s)y_m(s) + F(s)r_c(s) \tag{4}$$

where $u(s)$ is the control surface command vector, $K(s)y_m(s)$ is the feedback contribution, and $F(s)r_c(s)$ is the feedforward contribution.

The reference command vector is:

$$r_c(s) = \begin{bmatrix} \Phi_{ref}(s) \\ \beta_{ref}(s) \end{bmatrix} \tag{5}$$

where Φ_{ref} is the bank-angle reference and $\beta_{ref}$is the sideslip reference.

The sign convention associated with the feedback loops is embedded within the controller gains. The feedforward path shapes the pilot command before the flexible dynamics are excited, while the H_∞ feedback controller preserves closed-loop stability and provides disturbance rejection.

The overall flight control architecture includes actuator dynamics, sensor delays, and Butterworth filters for measurement-noise attenuation. The selected inner and middle ailerons are used for lateral control because their effectiveness remains consistent across the flight envelope, while the feedback and feedforward control structure together provide a means of balancing flying-quality requirements, structural load alleviation, and passenger ride comfort. The complete lateral–directional control

https://doi.org/10.71945/icas2026_0630

architecture for the flexible BWB aircraft is shown in Figure 4.

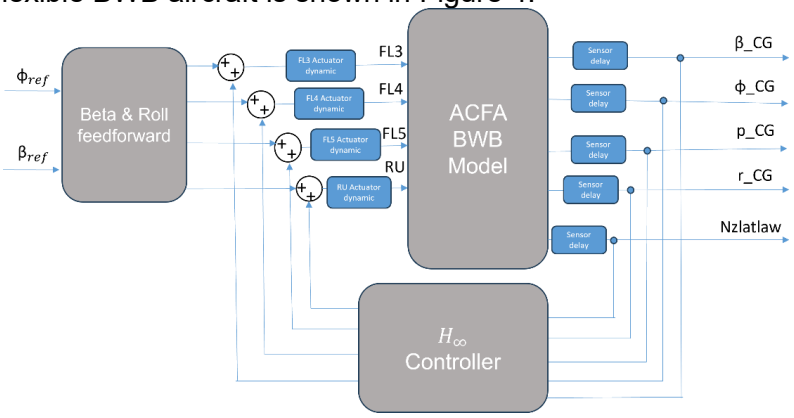


Figure 4. Lateral–directional flight control architecture for the flexible BWB aircraft [18].

3 Handling Qualities and Passenger Ride Comfort Assessment

3.1 Passenger Comfort Assessment Methodology

Passenger ride comfort was assessed using the BS 6841:1987 standard due to its suitability for multi-axial vibration assessment in aerospace applications [12]. Evaluations were performed at multiple passenger seating locations distributed throughout the cabin, as well as at the pilot station. For symmetric cabin locations, acceleration signals from the left and right passenger seats were averaged to obtain representative comfort metrics for each seating zone.

The acceleration experienced by a passenger depends not only on the aircraft centre-of-gravity motion, but also on the passenger location relative to the centre of gravity and the local flexible structural deformation. The acceleration at a passenger location (P) can be expressed as:

$$\mathrm{a}_P(t) = \mathrm{a}_{CG}(t) + \dot{\omega}(t) \times \mathrm{r}_P + \omega(t) \times (\omega(t) \times \mathrm{r}_P) + \mathrm{a}_{flex,P}(t) \tag{6}$$

where $\mathrm{a}_P(t)$ is the acceleration at passenger location P, $\mathrm{a}_{CG}(t)$is the acceleration at the aircraft centre of gravity, $\omega(t)$ is the angular velocity vector, $\dot{\omega}(t)$ is the angular acceleration vector, r_P is the position vector from the centre of gravity to the passenger location, and $\mathrm{a}_{flex,P}(t)$ is the local acceleration contribution due to structural flexibility. This relationship highlights why ride comfort can vary significantly across the BWB cabin, particularly at outboard and aft passenger locations.

For symmetric passenger locations, the left and right seat responses were averaged as:

$$\mathrm{a}_{zone}(t) = \frac{1}{2}\left[\mathrm{a}_{P,left}(t) + \mathrm{a}_{P,right}(t)\right] \tag{7}$$

where $\mathrm{a}_{zone}(t)$ is the representative acceleration response for the corresponding cabin zone.

Human sensitivity to vibration depends strongly on both vibration frequency and excitation direction. Consequently, the BS 6841 methodology applies direction-dependent frequency weightings to quantify human exposure to vibration and motion sickness effects. In the present study, two comfort criteria were considered: whole-body vibration exposure over the frequency range $0.5–80$ Hz, and low-frequency motion sickness sensitivity over the range $0.1–0.5$ Hz.

Frequency weighting filters W_b, W_d, and $W_e$were applied for the whole-body vibration assessment, while filter W_f was used for the motion sickness evaluation. The frequency-weighting characteristics used in the assessment are shown in Figure 5. The filters were implemented according to the specifications defined in BS 6841:1987. The frequency-weighted translational acceleration components may be written as:

$$\begin{aligned} \tilde{a}_x(t) &= W_d(s)a_x(t) \\ \tilde{a}_y(t) &= W_d(s)a_y(t) \\ \tilde{a}_z(t) &= W_b(s)a_z(t) \end{aligned} \tag{8}$$

where a_x, a_y, and a_z are the acceleration components in the longitudinal, lateral, and vertical directions,

https://doi.org/10.71945/icas2026_0630

respectively. The corresponding weighted rotational vibration components are given by:

$$\begin{aligned}\tilde{\alpha}_x(t) &= W_e(s)\alpha_x(t)\\ \tilde{\alpha}_y(t) &= W_e(s)\alpha_y(t)\\ \tilde{\alpha}_z(t) &= W_e(s)\alpha_z(t)\end{aligned} \tag{9}$$

where α_x, α_y, and α_z are the rotational vibration components about the three body axes.
For the whole-body vibration criterion, the weighted translational and rotational components were combined using the multiplying factors defined by BS 6841:

$$a_v(t) = \left[(k_x\tilde{a}_x)^2 + (k_y\tilde{a}_y)^2 + (k_z\tilde{a}_z)^2 + (k_r\tilde{\alpha}_x)^2 + (k_r\tilde{\alpha}_y)^2 + (k_r\tilde{\alpha}_z)^2\right]^{1/2} \tag{10}$$

where $a_v(t)$ is the combined weighted vibration signal, and k_x, k_y, k_z, and $k_r$are the multiplying factors specified by the standard.

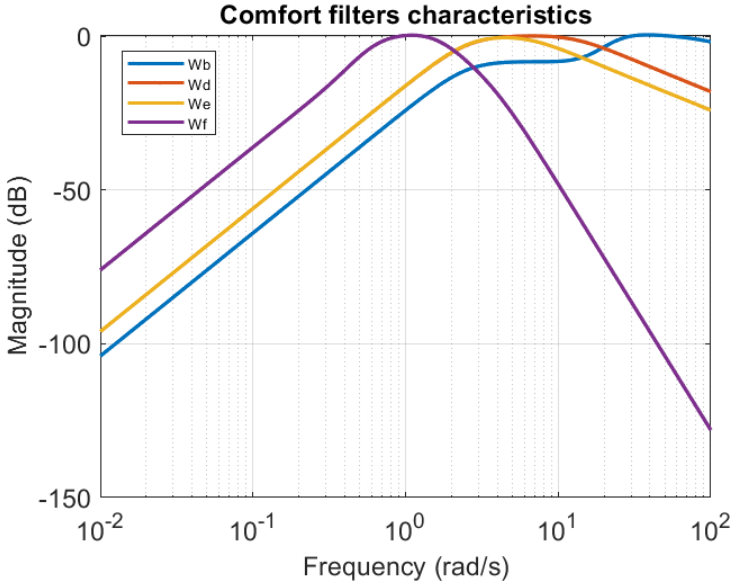


Figure 5. Frequency-weighting characteristics for comfort assessment as defined in BS 6841 [12].

In contrast, the motion sickness criterion considered only the low-frequency vertical acceleration component, consistent with the BS 6841 definition of low-frequency kinetosis response. The weighted motion sickness signal was therefore calculated as:

$$a_{ms}(t) = W_f(s)a_z(t) \tag{11}$$

where $a_{ms}(t)$ is the weighted motion sickness acceleration signal.
The filtered acceleration signals were subsequently processed using root mean square (RMS) calculations in order to quantify vibration exposure levels:

$$a_{RMS} = \sqrt{\frac{1}{T}\int_0^T a_w^2\,(t)\,dt} \tag{12}$$

where $a_w(t)$ represents the relevant weighted acceleration signal, either $a_v(t)$ for whole-body vibration or $a_{ms}(t)$ for motion sickness, and $T$is the assessment time interval. RMS metrics were selected due to their suitability for sustained vibration assessment under manoeuvre and gust conditions. The resulting weighted RMS values were compared against the comfort scale defined within BS 6841, shown in Figure 6, to classify the expected passenger comfort levels.

https://doi.org/10.71945/icas2026_0630

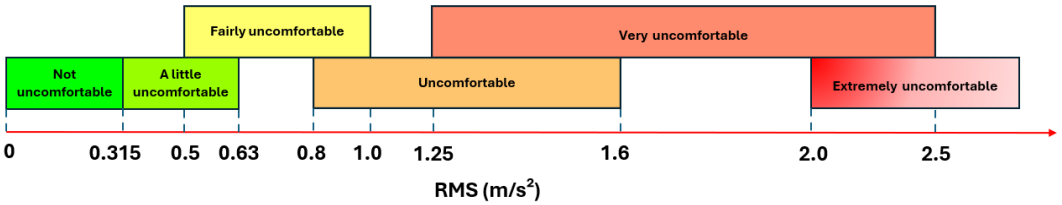


Figure 6. Vibration comfort scale according to BS-6841 [12].

3.2 Gust and Manoeuvre Scenarios

Atmospheric disturbances were modelled using a lateral one-minus-cosine gust profile applied as an exogenous disturbance at the aircraft centre of gravity. The lateral gust velocity was defined as:

$$v_g(t) = \frac{V_g}{2}\left[1 - \cos\left(\frac{2\pi t}{T_g}\right)\right], 0 \le t \le T_g$$
$$v_g(t) = 0, t < 0 \text{ or } t > T_g \tag{13}$$

where $v_g(t)$ is the lateral gust velocity, V_g is the peak gust velocity, and T_g is the gust duration. The gust duration was defined as a function of gust length and aircraft cruise speed as:

$$T_g = \frac{L_g}{U_0} \tag{14}$$

where L_g is the gust length and U_0 is the aircraft cruise speed. A peak gust velocity of $V_g = 19\ \mathrm{m/s}$ was selected to represent a severe lateral disturbance condition.

To identify a representative worst-case scenario for flexible structural excitation, multiple gust lengths were investigated. Comparisons between long- and short-duration gust inputs showed that shorter gust lengths generated significantly larger excitation of the dominant bending modes, as indicated by increased values of the antisymmetric wing acceleration parameter $N_{z_{lat.law}}$. Consequently, a gust length of $L_g = 45.72\ \mathrm{m}$ was selected for the present study as the critical disturbance condition. The influence of gust length on $N_{z_{lat.law}}$ is shown in Figure 7.

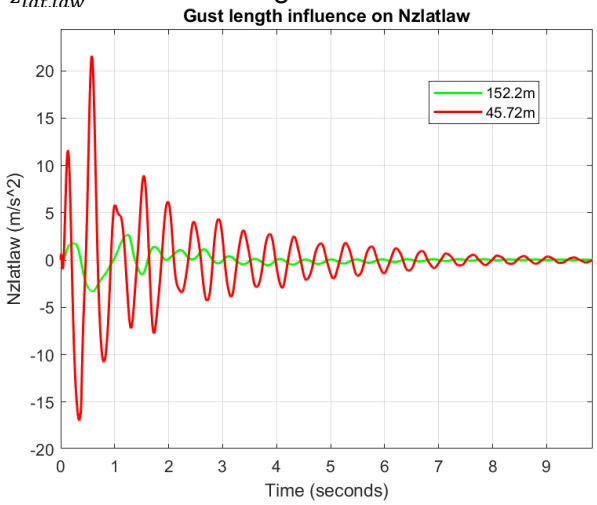


Figure 7. Influence of gust length on $N_{z_{lat.law}}$.

In addition to gust excitation, multiple bank-angle manoeuvre scenarios were evaluated to investigate the influence of rolling motion on passenger comfort. The manoeuvre severity was defined using the commanded bank-angle reference, ϕ_{cmd}:

$$\phi(t) \rightarrow \phi_{cmd}$$

The peak comfort-criterion values were evaluated for different commanded bank angles at a dynamic pressure of $Q = 22000\ \mathrm{Pa}$ and Mach number $M = 0.85$. The variation of peak comfort-criterion values with commanded bank angle is shown in Figure 8.

The analysis showed that bank-angle commands above approximately $42°$ resulted in RMS comfort levels entering the “fairly uncomfortable” region, particularly at outboard passenger locations. A $60°$ bank-angle manoeuvre was therefore selected as the representative worst-case operational scenario

https://doi.org/10.71945/icas2026_0630

due to its combination of significant structural excitation and operational relevance for emergency return-to-airport conditions:

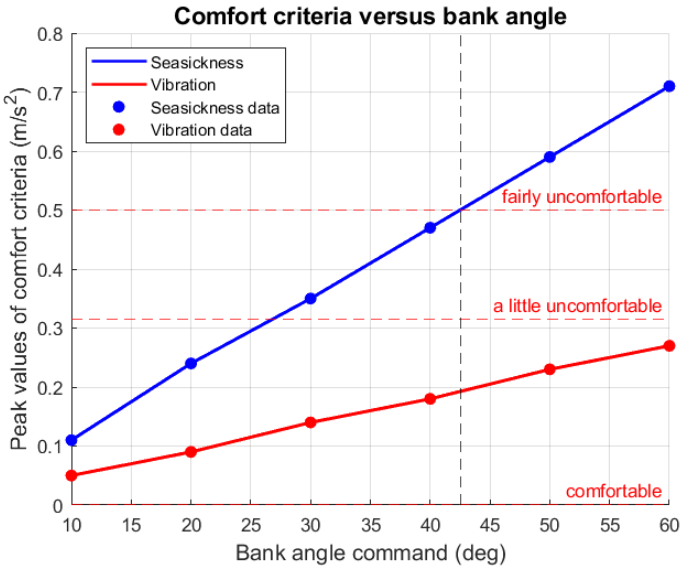


Figure 8. Peak comfort-criterion values for different commanded bank angles at dynamic pressure Q=22000 Pa and Mach number M=0.85.

4 Simulation Setup and Results

4.1 Definition of Critical Assessment Scenarios

The passenger comfort assessment was performed under a series of manoeuvre and disturbance conditions selected to represent critical operating scenarios for the flexible blended wing body aircraft. The objective was to evaluate the interaction between lateral–directional manoeuvres, gust-induced structural excitation, and passenger ride comfort throughout the distributed cabin.

The simulations were conducted using the flight configuration defined in the previous sections at a flight condition corresponding to a dynamic pressure of $Q = 22000$ Pa and a Mach number of $M = 0.85$. Passenger comfort was evaluated at multiple cabin locations using the BS 6841 vibration assessment methodology.

An initial investigation considered the aircraft response to an isolated lateral gust disturbance in cruise conditions. The atmospheric disturbance was modelled using a one-minus-cosine lateral gust profile with a peak velocity of 19 m/s applied at the aircraft centre of gravity. Multiple gust lengths were investigated in order to identify the disturbance condition producing the strongest flexible structural excitation. Comparisons between gust lengths of 152.2 m and 45.72 m showed that the shorter gust generated significantly larger excitation of the dominant antisymmetric bending modes, as indicated by the increased $N_{z_{lat.law}}$ response. Consequently, the 45.72 m gust length was selected as the representative worst-case disturbance condition for the remainder of the study.

Following the isolated gust analysis, combined manoeuvre-and-disturbance scenarios were investigated. A commanded 60° bank-angle manoeuvre was selected as the primary assessment case due to its operational relevance for emergency return-to-airport situations and its strong excitation of the flexible aircraft dynamics. As shown in Figure 8, bank-angle commands above approximately $42°$caused the RMS comfort levels to enter the “fairly uncomfortable” region, particularly at outboard passenger locations. The $60°$bank-angle manoeuvre was therefore selected as a representative critical case for assessing both handling qualities and passenger ride comfort.

In addition to the nominal flight condition, the influence of aircraft centre-of-gravity position and fuel loading on passenger comfort was also investigated to evaluate the sensitivity of the flexible response to variations in mass distribution throughout the flight envelope.

4.2 Gust-Induced Flexible Aircraft Response

The flexible response of the ACFA 2020 blended wing body aircraft was assessed using the antisymmetric wing acceleration parameter $N_{z_{lat.law}}$, which provides a direct measure of the excitation of the antisymmetric bending modes during lateral–directional manoeuvres and atmospheric disturbances. This parameter is particularly suitable for evaluating the interaction between roll motion and flexible structural dynamics, as it captures the difference between the vertical accelerations at the

https://doi.org/10.71945/icas2026_0630

left and right wingtips.
A comparison between the nominal 60° bank-angle manoeuvre and the same manoeuvre combined with a lateral gust disturbance shows that the atmospheric disturbance significantly amplifies the flexible structural response. In particular, the lateral gust strongly excites the dominant bending modes of the aircraft, resulting in substantially larger oscillations of the $N_{z_{lat.law}}$ parameter compared with the clean manoeuvre case. The corresponding comparison of $N_{z_{lat.law}}$ is shown in Figure 9.

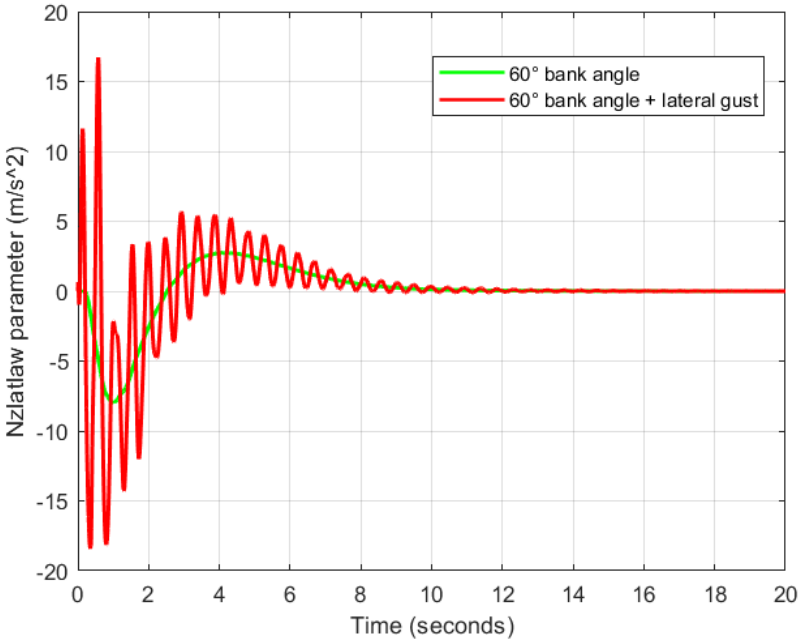


Figure 9. Comparison of $N_{z_{lat.law}}$ for the clean $60°$ bank-angle manoeuvre and the combined $60°$ bank-angle manoeuvre with lateral gust disturbance.

The increased oscillatory response demonstrates the strong sensitivity of the flexible BWB configuration to lateral atmospheric disturbances. Although the commanded roll manoeuvre alone generates moderate antisymmetric structural excitation, the addition of the lateral gust produces significantly larger dynamic wing deformation and prolonged flexible oscillations. This behaviour highlights the strong coupling between lateral–directional aircraft motion and aeroelastic response in large flexible tailless aircraft configurations.
The results also indicate that short-duration gust disturbances are particularly critical for exciting the flexible structural modes. As discussed previously, the selected 45.72 m gust length generated larger antisymmetric bending responses than longer gust disturbances, confirming that sharper atmospheric disturbances contain frequency content closer to the dominant structural modes of the aircraft. These amplified structural oscillations directly influence the passenger vibration environment throughout the distributed cabin and therefore play a key role in the subsequent ride comfort assessment.

4.3 Passenger Ride Comfort Assessment

4.3.1 *Motion Sickness Assessment*

Passenger exposure to low-frequency motion associated with motion sickness was evaluated using the BS 6841 motion sickness criterion over the frequency range 0.1–0.5 Hz. The assessment revealed significant spatial variations in comfort levels throughout the cabin under the combined 60° bank-angle manoeuvre and lateral gust disturbance scenario.
The RMS values obtained for the worst-case condition indicate that the rear–outer, middle–outer, and middle–inner passenger locations enter the “fairly uncomfortable” region according to the BS 6841 comfort scale. In contrast, passengers located in the front–centre and middle–centre regions remain within the comfortable range, while the rear–inner region approaches the discomfort threshold. The pilot station showed negligible motion sickness levels due to the reduced low-frequency vertical acceleration response at that location. The motion sickness assessment for this case is shown in Figure 10.

https://doi.org/10.71945/icas2026_0630

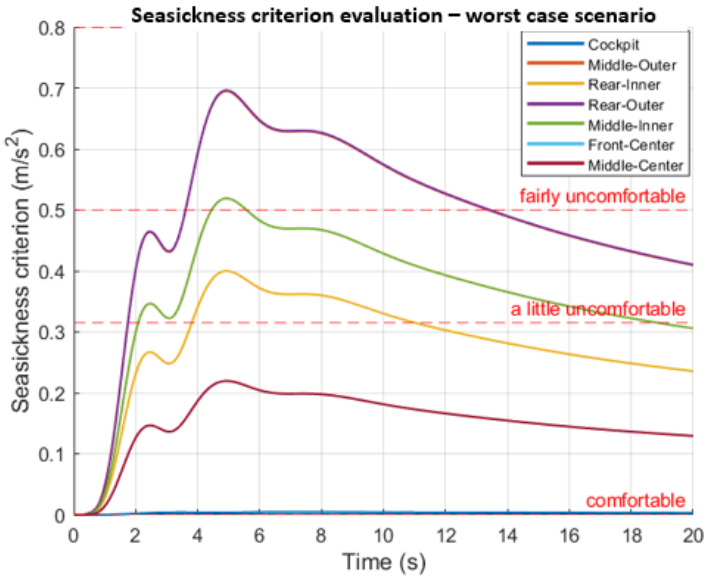


Figure 10. Motion sickness criterion for the combined 60° bank-angle manoeuvre and 45.72 m lateral gust disturbance at Q=22000 Pa and M=0.85.

The results demonstrate that low-frequency passenger comfort is strongly influenced by cabin position within the flexible lifting surface. Outboard and aft cabin regions experience larger low-frequency accelerations due to increased structural deformation and higher participation of the flexible bending modes during gust excitation.

4.3.2 *Whole-Body Vibration Assessment*

The whole-body vibration assessment was performed over the frequency range 0.5–80 Hz using the BS 6841 weighted RMS criterion. Compared with the motion sickness results, the vibration criterion revealed more pronounced vibration exposure throughout several cabin regions and at the cockpit location. The rear–outer, middle–inner, middle–centre, and cockpit locations reached vibration levels classified as uncomfortable according to the BS 6841 standard. In contrast, the front–centre and rear–inner cabin regions exhibited comparatively lower vibration levels. The whole-body vibration assessment is shown in Figure 11.

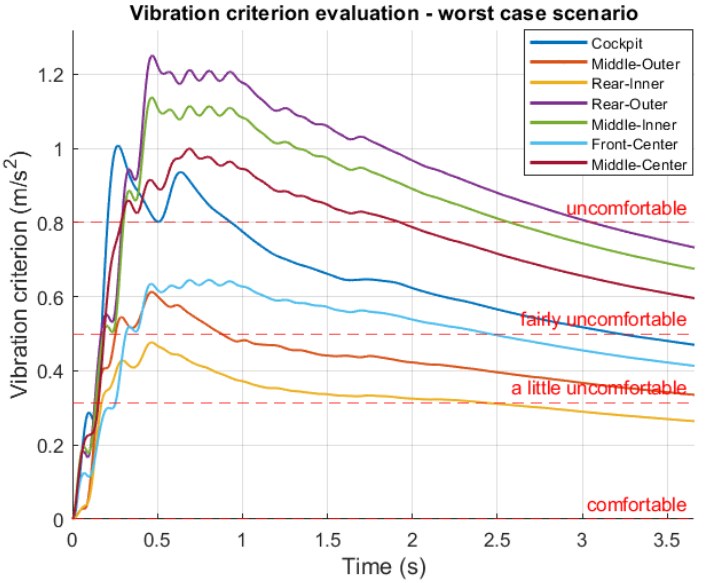


Figure 11. Whole-body vibration criterion for the combined $60°$bank-angle manoeuvre and 45.72 m lateral gust disturbance at $Q = 22000$ Pa and $M = 0.85$ at various locations.

The higher-frequency vibration exposure is primarily associated with excitation of the dominant flexible structural modes during the combined manoeuvre and gust disturbance. The results highlight the strong spatial variability of passenger ride comfort within flexible BWB aircraft and demonstrate the increased sensitivity of outboard passenger locations to gust-induced structural excitation.

https://doi.org/10.71945/icas2026_0630

4.3.3 Influence of Flight Conditions

In addition to the worst-case manoeuvre and gust scenario, the influence of flight condition parameters was investigated to assess the sensitivity of passenger ride comfort to changes in aircraft configuration. In particular, variations in centre-of-gravity position and fuel loading were considered, as these parameters affect the aircraft mass distribution, rigid-body dynamics, and flexible structural response. First, the influence of centre-of-gravity position was assessed by comparing two configurations during a 60° bank-angle manoeuvre. The rear centre-of-gravity case was located at $CG_x = 26\text{m}$, while the forward case was located at $CG_x = 23.67\text{m}$. The results indicate that centre-of-gravity position has a measurable but relatively modest influence on the antisymmetric wing acceleration response. The rear centre-of-gravity case produced slightly larger $N_{z_{lat.law}}$ values, indicating increased excitation of the antisymmetric flexible modes. The effect of centre-of-gravity position on $N_{z_{lat.law}}$ is shown in Figure 12.

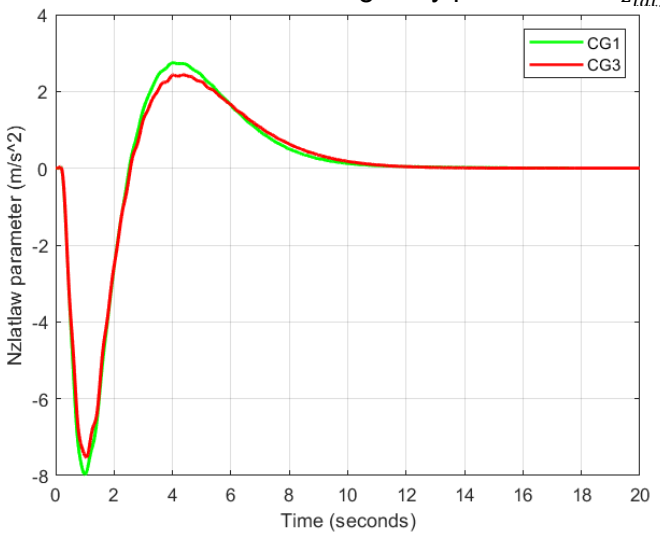
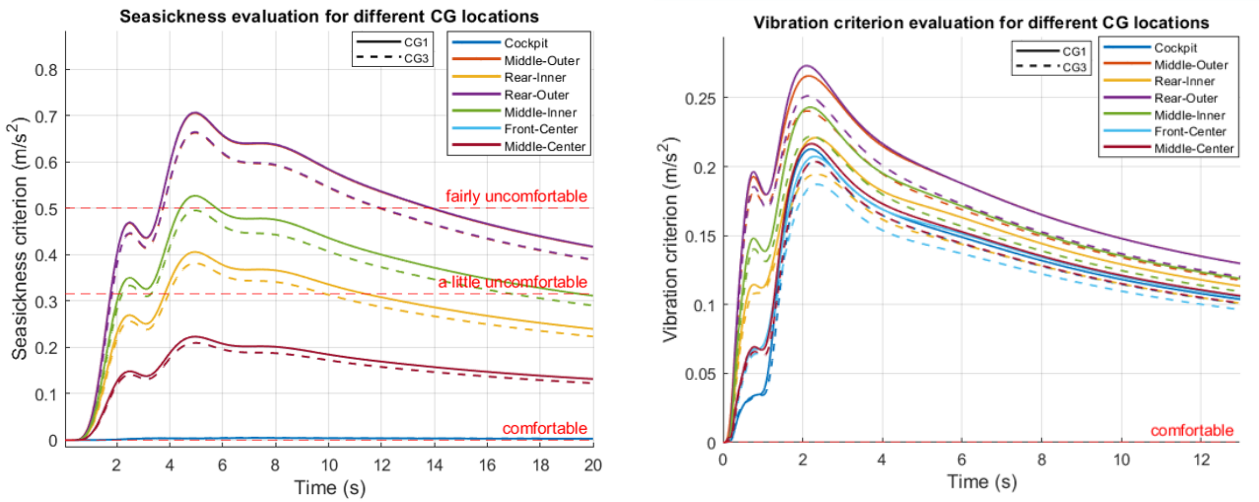


Figure 12. Comparison of the antisymmetric wing acceleration parameter $N_{z_{lat.law}}$ for different centre-of-gravity positions during a 60°bank-angle manoeuvre. $CG1 = 26\text{ m}$ represents the aft centre-of-gravity position, while $CG3 = 23.67\text{ m}$ represents the forward centre-of-gravity position.

The corresponding comfort assessment showed that changes in centre-of-gravity position produced variations in both the motion sickness and whole-body vibration criteria. Although the overall comfort trends remained similar, the results suggest that mass distribution and trim condition can influence the level of vibration exposure experienced by passengers. The corresponding comfort metrics for the two centre-of-gravity positions are shown in Figure 13.



(a) Motion sickness (b) Vibration criteria

Figure 13. Comparison of motion sickness and whole-body vibration criteria for forward (CG3) and aft (CG1) centre-of-gravity positions during a 60° bank-angle manoeuvre.

The influence of fuel loading was also assessed by comparing a fully loaded configuration with an

https://doi.org/10.71945/icas2026_0630

almost-empty fuel-load case during the same 60° bank-angle manoeuvre. The difference in aircraft mass between the two cases was approximately 51029 kg. The almost-empty configuration produced slightly higher $N_{z_{lat.law}}$ values and increased RMS values for the low-frequency motion sickness criterion, indicating that passengers may experience greater susceptibility to discomfort towards the end of flight. The influence of fuel loading on $N_{z_{lat.law}}$ is shown in Figure 14.

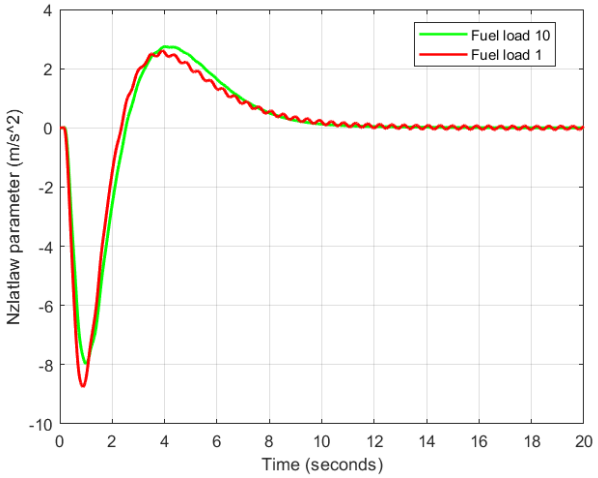
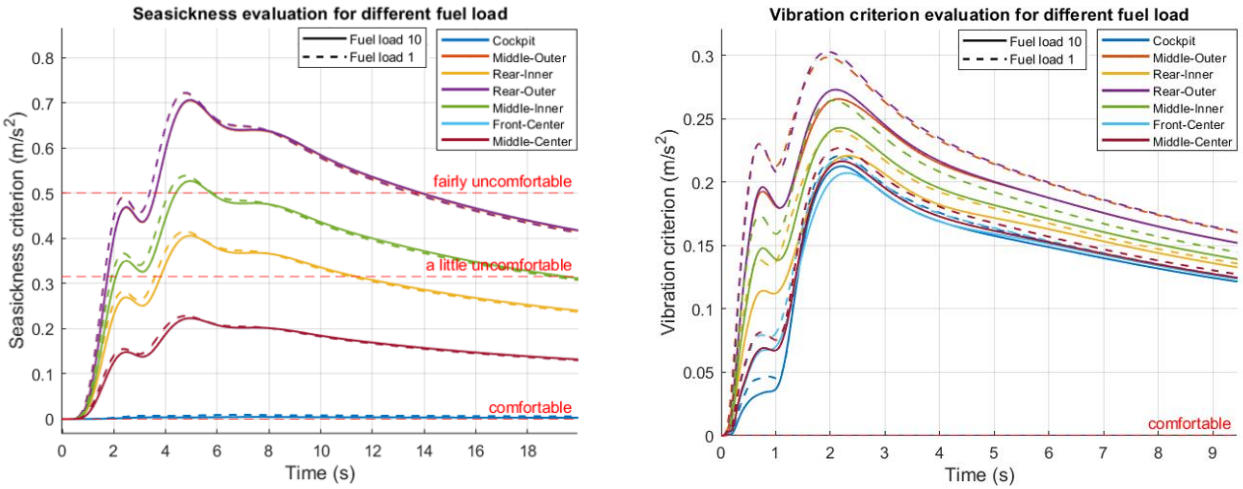


Figure 14. Comparison of the antisymmetric wing acceleration parameter $N_{z_{lat.law}}$ for different fuel-load configurations during a $60°$ bank-angle manoeuvre. Fuel Load 10 represents the fully loaded aircraft, while Fuel Load 1 represents the near-empty fuel configuration.

The corresponding comfort metrics for the fuel-load cases are shown in Figure 15. For the whole-body vibration criterion, the almost-empty configuration also showed increased vibration levels, although the values remained within the acceptable comfort range for the manoeuvre considered. These results indicate that variations in mass distribution and fuel loading can influence passenger comfort, but their effect is less dominant than the combined influence of large lateral manoeuvres and gust-induced flexible excitation.



(a) Motion sickness criterion. (b) Whole-body vibration criterion.

Figure 15. Comparison of motion sickness and whole-body vibration criteria for different fuel-load cases during a $60°$ bank-angle manoeuvre. Fuel Load 10 represents the fully loaded aircraft, while Fuel Load 1 represents the near-empty fuel configuration.

4.4 Discussion

The results demonstrate the strong interaction between lateral–directional manoeuvres, flexible structural dynamics, and passenger ride comfort within large, blended wing body aircraft. Unlike conventional tube-and-wing configurations, where most passengers are located close to the fuselage centreline, the distributed cabin arrangement of the BWB exposes passengers to significantly different vibration environments depending on their position within the lifting surface.

The outboard passenger locations consistently exhibited the highest discomfort levels for both the

https://doi.org/10.71945/icas2026_0630

motion sickness and whole-body vibration criteria. This behaviour is primarily associated with the larger structural deformation amplitudes occurring farther from the aircraft centreline, where the influence of the dominant bending modes becomes more significant. Consequently, atmospheric disturbances and rolling manoeuvres generate substantially larger acceleration levels at the outer cabin regions compared with the centre-body locations.

The results further highlight the strong sensitivity of flexible BWB aircraft to lateral gust excitation. While the nominal 60° bank-angle manoeuvre already produces noticeable structural excitation, the addition of a lateral gust disturbance significantly amplifies the antisymmetric bending response, as reflected by the increased $N_{z_{lat.law}}$ oscillations. Short-duration gusts were found to be particularly critical because their frequency content lies closer to the dominant flexible structural modes of the aircraft.

An important observation from the present study is the trade-off between manoeuvrability and passenger comfort. The lateral–directional controller intentionally employed a relatively slow roll response to reduce structural excitation and mitigate passenger acceleration levels throughout the cabin. Although this strategy relaxes conventional roll agility requirements associated with MIL-F-8785C criteria, it provides substantial benefits in terms of ride comfort and structural load reduction for flexible transport aircraft.

The influence of centre-of-gravity position and fuel loading further demonstrates the sensitivity of passenger comfort to aircraft mass distribution. Although these effects were less dominant than the combined manoeuvre-and-gust excitation, changes in aircraft loading conditions still modified the flexible structural response and corresponding vibration levels experienced throughout the cabin.

Overall, the study demonstrates that passenger ride comfort should be considered as an integrated design driver for future blended wing body aircraft. The strong coupling between active flight control, aeroelastic response, and distributed passenger exposure suggests that future flexible transport aircraft may require multidisciplinary optimization approaches combining structural design, control synthesis, and cabin-layout considerations in order to simultaneously satisfy flying qualities, structural load alleviation, and passenger comfort requirements.

5 Conclusions

This paper investigated the lateral–directional flying qualities and passenger ride comfort characteristics of the ACFA 2020 flexible blended wing body aircraft under representative manoeuvre and atmospheric disturbance conditions. A robust H_∞-based feedback controller combined with a feedforward load alleviation strategy was assessed using nonlinear simulations including coupled rigid-body and flexible structural dynamics.

The results demonstrated that lateral gust disturbances significantly amplify the antisymmetric bending response of the aircraft, particularly during combined manoeuvre-and-gust scenarios. The selected worst-case condition, consisting of a 60° bank-angle manoeuvre combined with a 45.72 m lateral gust disturbance, produced substantial excitation of the dominant flexible structural modes, leading to increased passenger vibration exposure throughout the distributed cabin.

Passenger ride comfort assessments performed using the BS 6841 standard revealed strong spatial variations in comfort levels across the aircraft. Outboard and aft passenger locations consistently exhibited the highest discomfort levels for both the motion sickness and whole-body vibration criteria due to their increased sensitivity to flexible structural deformation. In contrast, centre-body cabin locations experienced significantly lower vibration exposure.

The study also highlighted the trade-off between manoeuvrability and passenger comfort in flexible transport aircraft. The relatively slow roll response adopted within the active control framework reduced structural excitation and passenger acceleration levels, although at the expense of conventional roll agility requirements. Furthermore, variations in centre-of-gravity position and fuel loading were shown to influence the flexible response and resulting comfort metrics, although to a lesser extent than gust-induced excitation.

Overall, the results demonstrate that passenger ride comfort should be considered as an integrated design driver for future blended wing body aircraft. The strong coupling between active flight control, aeroelastic response, and distributed passenger vibration exposure suggests that future flexible transport aircraft will require multidisciplinary design approaches combining structural optimization, active control synthesis, and cabin-layout considerations to simultaneously satisfy flying qualities, structural load alleviation, and ride comfort requirements.

https://doi.org/10.71945/icas2026_0630

6 Acknowledgements

The authors gratefully acknowledge the contributions of the ACFA 2020 consortium to the development of the blended wing body aircraft model and active control framework used in this study. The original ACFA 2020 project was supported under the European Union Seventh Framework Programme (FP7). The authors also acknowledge the use of modelling and control material reported in previous ACFA-related work, particularly the BWB aircraft model and control architecture documented by Kozek and Schirrer. This paper further builds on MSc thesis work carried out at Cranfield University on lateral–directional handling qualities and passenger ride comfort assessment of the ACFA 2020 BWB configuration.

7 Contact Author Email Address

Mailto: mushfiqul.alam@cranfield.ac.uk

8 Copyright Statement

The authors confirm that they, and/or their company or organization, hold copyright on all of the original material included in this paper. The authors also confirm that they have obtained permission, from the copyright holder of any third-party material included in this paper, to publish it as part of their paper. The authors confirm that they give permission or have obtained permission from the copyright holder of this paper, for the publication and distribution of this paper as part of the ICAS proceedings or as individual off prints from the proceedings.

References

[1] Westwood, M., “Sustainability,” 2024.

[2] Airbus, “ZEROe: Our Hydrogen-Powered Aircraft.”

[3] Hasan, Y. J., Schwithal, J., Pfeiffer, T., Liersch, C. M., and Looye, G., “Handling Qualities Assessment of a Blended Wing Body Configuration under Uncertainty Considerations,” Deutsche Gesellschaft für Luft- und Raumfahrt-Lilienthal-Oberth eV, 2018.

[4] Kozek, M., and Schirrer, A., “Modeling and Control for a Blended Wing Body Aircraft: A Case Study,” Springer, 2015. https://doi.org/10.1007/978-3-319-10792-9

[5] Wang, L., Zhang, N., Liu, H., and Yue, T., “Stability Characteristics and Airworthiness Requirements of Blended Wing Body Aircraft with Podded Engines,” *Chinese Journal of Aeronautics*, Vol. 35, No. 6, 2022, pp. 77–86. https://doi.org/10.1016/j.cja.2021.09.002

[6] Castro, H. V, “Flying and Handling Qualities of a Fly-by-Wire Blended-Wing-Body Civil Transport Aircraft,” Cranfield University, 2003.

[7] Thorpe, A. W., and Curtis, M. F., “Lateral Stability of Tailless Aircraft,” *Aeronautical Council Report and Memoranda*, 1943. https://reports.aerade.cranfield.ac.uk/handle/1826.2/3210

[8] Aerospace, and of Europe (ASD), D. I. A., “Latest ACARE Documents.”

[9] Mansfield, N. J., “Human Response to Vibration,” CRC Press, 2004. https://doi.org/10.1201/b12481

[10] DeHart, R. L., “Health Issues of Air Travel,” *Annual review of public health*, Vol. 24, 2003, pp. 133–151. https://doi.org/10.1146/annurev.publhealth.24.100901.140853

[11] International Organization for Standardization, “ISO 2631-1:1997 Mechanical Vibration and Shock – Evaluation of Human Exposure to Whole-Body Vibration – Part 1: General Requirements.”

[12] BSI, “Guide to Measurement and Evaluation of Human Exposure to Whole-Body Mechanical Vibration and Repeated Shock.”

[13] Paddan, G. S., and Griffin, M. J., “Evaluation of Whole-Body Vibration in Vehicles,” *Journal of Sound and Vibration*, Vol. 253, No. 1, 2002, pp. 195–213. https://doi.org/https://doi.org/10.1006/jsvi.2001.4256

[14] Wildschek, A., Havar, T., and Plötner, K., “An All-Composite, All-Electric, Morphing Trailing Edge Device for Flight Control on a Blended-Wing-Body Airliner,” *Proceedings of the Institution of Mechanical Engineers, Part G: Journal of Aerospace Engineering*, Vol. 224, No. 1, 2010, pp. 1–9. https://doi.org/10.1243/09544100JAERO622

[15] Alam, M., and Hromcik, M., “Structural Load Alleviation Using Distributed Delay Shaper: Application to Flexible Aircraft,” *Control Engineering Practice*, Vol. 89, 2019. https://doi.org/10.1016/j.conengprac.2019.05.005

[16] Alam, M., Hromcik, M., and Hanis, T., “Active Gust Load Alleviation System for Flexible Aircraft: Mixed Feedforward/Feedback Approach,” *Aerospace Science and Technology*, Vol. 41, No. 1, 2015, pp. 122–133. https://doi.org/10.1016/j.ast.2014.12.020

[17] Carpman, N., Standard, I., Impact, I., Control, F., Design, S., Dillsaver, M. J., Cesnik, C. E. S., Kolmanovsky, I. V, Wildschek, A., Maier, R., Hromcik, M., Characteristics, L. S., Dc, W., Dogan, A., Lewis, T. A., Blake, W., Eger, T., Kociolek, a, Dickey, J. P., and Lewis, T. A., “Hybrid Controller for Gust Load Alleviation and Ride Comfort Improvement Using Direct Lift Control Flaps,” *Proceedings of Third …*, Vol. 3, No. 6, 2008, pp. 101–102. https://doi.org/doi:10.2514/6.2011-6368

[18] Renault, J., “Lateral-Directional Handling and Flying Qualities Assessment of a Blended Wing Body (BWB) ACFA 2020 Configuration,” Cranfield University, Cranfield, Bedford, 2025.